
CHEMICAL PHYSICS
OF ATMOSPHERIC PHENOMENA

Emissivity of the Main Greenhouse Gases

A. E. Galashev and O. R. Rakhmanova

Institute of Industrial Ecology, Ural Branch, Russian Academy of Sciences, Yekaterinburg, Russia

e-mail: galashev@ecko.uran.ru

Received July 6, 2012

Abstract—Based on the high-resolution data on the absorption lines of gases from the HITRAN open international database in conjunction with inverse Fourier transform, the autocorrelation function of the total dipole moment of the molecules of the main greenhouse gases, such as H₂O, CO₂, O₃, N₂O, and CH₄, are determined. The spectral absorption coefficient and spectral radiance of these gases in the investigated IR region is calculated. An analysis of the emissivity of each of the gases is performed. An efficiency criterion of IR absorption and emission is introduced, according to which the studies gases are ranked.

Keywords: greenhouse gases, absorption and emission spectra, efficiency criterion of IR absorption and emission

DOI: 10.1134/S1990793113030020

INTRODUCTION

Long-wave radiation from the Earth's surface is absorbed and reemitted in the atmosphere by greenhouse gases, clouds, aerosols, and clusters. The characteristics of energy transfer depend on the temperature and the ability of the gas to absorb radiation at a given wavelength. The greenhouse gases, which include water vapor, carbon dioxide, ozone, methane and nitrous oxide, play a key role in regulating the energy balance of the Earth's atmosphere. In the presence of clouds, the energy transfer depends on their number and the efficiency with which they absorb and reemit long-wave radiation. The radiation forcing F for a clear and cloudy sky differs substantially.

The concept of radiative forcing [1] is closely associated with studying the energy balance of the Earth's atmosphere, determined by the difference between the amounts of infrared radiation absorbed and emitted by the gases. This change in the balance is due to various factors. The unit of measurement of the radiative forcing is W/m². A positive value of F is indicative of an overall heating of the Earth's surface, whereas a negative one, cooling. The value of F , for example, for carbon dioxide CO₂, can be calculated by the formula [2]

$$F_{\text{CO}_2} = 5.35 \ln \left(\frac{C}{C_0} \right),$$

where C is the CO₂ concentration in ppm and $C_0 = 278$ ppm is a constant. At the current average CO₂ concentration of 387 ppm [3], the radiative forcing for it is $F_{\text{CO}_2} = 1.77$ W/m². For methane and nitrous oxide, the values of the radiative forcing, having a more complex functional dependence, are $F_{\text{CH}_4} = 0.48$ W/m²

and $F_{\text{N}_2\text{O}} = 0.16$ W/m², respectively. The stratospheric ozone is characterized by a negative radiative forcing, $F_{\text{O}_3}^{\text{str}} = -0.05$ W/m², indicating that it produces a cooling effect, while for the tropospheric ozone $F_{\text{O}_3}^{\text{tr}} = 0.35$ W/m² (in this case, ozone acts as a greenhouse gas). The total radiative forcing from all anthropogenic sources is 1.6 W/m² [4].

The method of instantaneous normal modes [5, 6], used for processing experimental data, gives an instantaneous picture of the scattering process. The latter may reflect the structure and dynamics of both equilibrium and nonequilibrium states. The measured state of a real physical system corresponds to the global minimum of the potential energy or to the lowest of the local minima for a nonequilibrium state of the system. In the case of absorption of infrared radiation, the spectrum of ideal states obtained in this manner will be denoted by $\sigma_{i_0}(\omega)$. Note that the HITRAN database is presented in the form of $\sigma_{i_0}(\omega)$ spectra. Because of time constraints and a limited number of selected configurations, the Monte Carlo and molecular dynamics methods do not enable to fully achieve a state characterized by the global minimum of the potential energy. Consequently, there are modes in the model that represent unstable transitions over an energy barrier. Such transitions occur in the real Earth's atmosphere. In this case, their origin is related to the instability of the processes occurring in the atmosphere. This is reflected in the multidimensional potential energy surface in the form of a negative curvature of its dependence on certain degrees of freedom. In other words, modes with imaginary frequencies appear. These modes are normally ignored or imitated by an exponentially decaying term, a

replacement leading to a structural relaxation. The IR absorption spectrum in the presence of transient modes will be designated as $\sigma(\omega)$. This spectrum is more accurately reflects the real picture of the scattering of radiation in the Earth's atmosphere because of a large number of complex physicochemical processes occurring in it.

The aim of this work is to review and analyze the radiative properties of the main greenhouse gases (H_2O , CO_2 , O_3 , N_2O , CH_4) on the basis of the experimental data collected in the HITRAN open international database, to obtain the infrared spectral radiance, and to rank these greenhouse gas according to the efficiency criterion of IR absorption and emission.

CALCULATION PROCEDURE

Determination of the spectral radiance of greenhouse gases and their emissivity are based on solving the inverse problem, more specifically, calculating the autocorrelation function of the total dipole moment of the molecule from the IR absorption spectra presented in the HITRAN database [7] by using Fourier transform. This database contains a set of bands represented in the form of absorption intensities expressed in $\text{cm}^{-1}/(\text{molecule cm}^{-2})$ units. Here, the frequency is expressed in cm^{-1} and the scattering cross section, in cm^2 , with normalization done per molecule. This set covers a wide frequency range (from 0 to 5000 cm^{-1}) with a $0.001\text{--}0.01 \text{ cm}^{-1}$ discretization. We selected a frequency range of $0 \leq \omega \leq 3600 \text{ cm}^{-1}$, because the intensity of the emission spectrum of the Earth's at 3600 cm^{-1} is less than 0.1% of its maximum intensity. The initial data file contained between 60000 (N_2O) and 125000 (CO_2) values. Data sampling was performed for the main isotope. The spectrum of bands for each frequency interval was transformed into the autocorrelation function separately, since in some cases, the spectra had a variable frequency step.

The autocorrelation function $F(t)$ of the total dipole moment of the molecule can be calculated using the Fourier transform as [8]

$$F(t) = \langle \mathbf{M}(t)\mathbf{M}(0) \rangle = \langle \mathbf{M}_i\mathbf{M}_i \rangle + k_B T \int_{-\infty}^{\infty} \sigma_{i\omega}(\omega) \cos(\omega t) d\omega,$$

where $\mathbf{M}(t)$ is the sum of the actual dipole moments of individual molecules at time t , \mathbf{M}_i is the value of \mathbf{M} at the potential minimum of mode i ; k_B is the Boltzmann constant, T is the temperature corresponding to the tropospheric or stratospheric conditions, and ω is the frequency of the absorbed electromagnetic wave. The first term on the right side of the equation can be neglected, since its contribution for nonzero frequencies is insignificant [8]. The density of states at all frequencies is positive.

Table 1. Concentration and average number \bar{n} of molecules in the 40-km near-ground layer

Molecule	Concentration, ppm	\bar{n} , 10^{40}
H_2O	10200	107.7
CO_2	387	4.0
CH_4	1.8	0.028
N_2O	0.32	0.0033
O_3	0.1–10	0.0010–0.1

Water vapor is the primary natural greenhouse gas, which accounts for more than 60% of the greenhouse effect. Moisture is transported into the atmosphere by evaporation from the Earth's surface, with ~90% of it being concentrated in the lower five-kilometer layer. The water vapor concentration decreases rapidly with increasing height. The amount of water contained in the atmosphere reaches $1.325 \cdot 10^{13}$ tons. Although the atmosphere extends upward for hundreds of kilometers, most of the air is concentrated in a thin layer. Half the mass of the atmosphere is located between the sea level and a height of 5–6 km, 90%, in a layer of up to 16 km, and 99%, in a layer of up to 30 km. The average concentrations (in ppm) of H_2O , CO_2 , CH_4 , N_2O , and O_3 in a 40-km layer of the Earth's atmosphere are listed in Table 1. The concentration of ozone near the Earth's surface can reach 0.1 ppm, increasing up to ~10 ppm at altitudes of 10–35 km, in the main ozone layer. Thus, the total concentration of all the gases examined here does not exceed 1.1%. The total mass of the atmosphere is $5.14 \cdot 10^{18}$ kg. The average molar weight of air is 29 g/mol. Then, the total number of molecules in the atmosphere is $1.067 \cdot 10^{44}$, while a 40-km-thick layer contains $\sim 1.056 \cdot 10^{44}$ molecules. The estimated number of molecules of greenhouse gases, as determined in accordance with their average concentration is given in Table 1.

CALCULATION OF THE SPECTRAL CHARACTERISTICS OF THE GASES

The intensity of the IR spectrum bands is determined by the Bouguer–Lambert–Beer law

$$I = I_0 e^{-\alpha l},$$

where α is the absorption coefficient and l is the thickness of the absorbing substance layer. In the SI system, the absorption coefficient is the reciprocal of the thickness of a substance that e -fold reduces the intensity of the monochromatic light passing through it. The lower the coefficient $e \alpha$, the higher the intensity of experimentally recorded IR spectra. Laboratory spectra provide information on the characteristic absorption frequencies and relative intensities of the spectra of various gases. A parameter more informative for numerical estimates and physical characteriza-

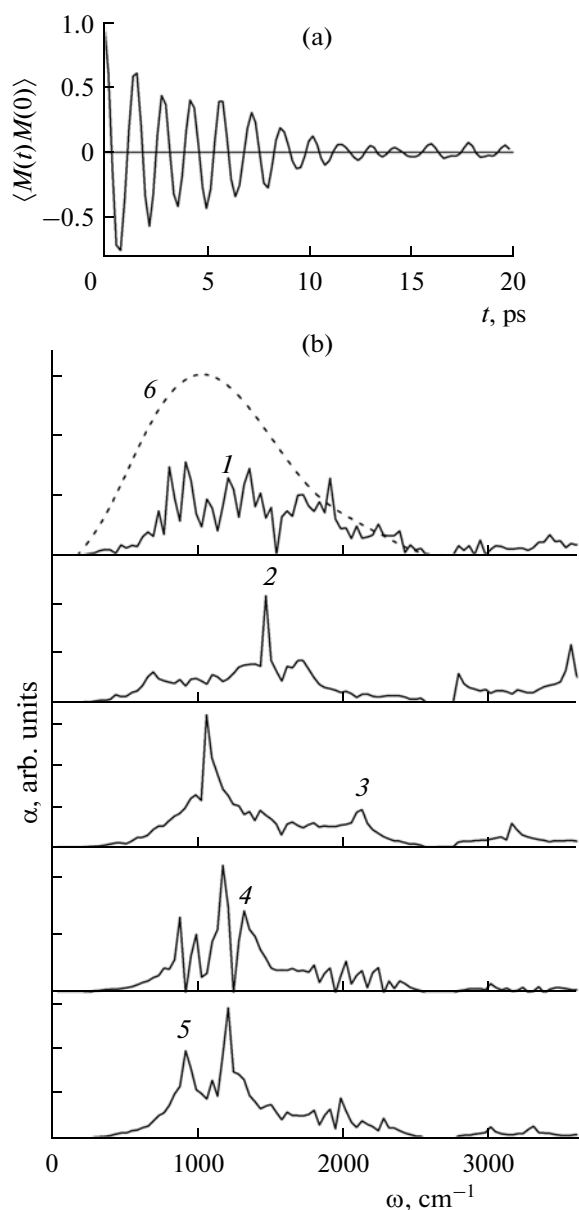


Fig. 1. (a) Reconstructed autocorrelation function of the total dipole moment of the N_2O molecule; (b) infrared spectral absorption coefficients of the greenhouse gases: (1) H_2O , (2) CO_2 , (3) O_3 , (4) CH_4 , and (5) N_2O ; (6) Earth's thermal radiation spectrum at $T = 280$ K.

tion of absorbing media is the spectral absorption coefficient $\alpha(\omega)$. It is used as an absolute characteristic of radiation absorption of by the medium. Given that the same gases in laboratory facilities and in the real atmosphere are fundamentally different media, their IR spectra can differ significantly. The IR spectra of the studied gases in the atmosphere can be more abundant because of their chemical reactions and interaction with atmospheric moisture, as well as due to the presence of contributions from other compo-

The imaginary part $\varepsilon''(\omega)$ of the dielectric permittivity is given by [9]

$$\begin{aligned} \frac{\varepsilon(\omega) - 1}{\varepsilon_0 - 1} &= - \int_0^{\infty} \exp(-i\omega t) \frac{dF}{dt} dt \\ &= 1 - i\omega \int_0^{\infty} \exp(-i\omega t) F(t) dt, \end{aligned}$$

where ε_0 is the static relative permittivity.

The IR absorption coefficients α of the studied greenhouse gases are also expressed through the imaginary part of $\varepsilon(\omega)$ [10]:

$$\alpha(\omega) = 2 \frac{\omega}{c} \text{Im} [\varepsilon(\omega)^{1/2}],$$

where c is the speed of light.

The IR spectral radiance is expressed through the imaginary part of the complex frequency-dependent dielectric permittivity, $\varepsilon(\omega) = \varepsilon'(\omega) - i\varepsilon''(\omega)$ as [11]

$$P = \frac{\varepsilon'' \langle E^2 \rangle \omega}{4\pi},$$

where $\langle E^2 \rangle$ is the mean square of the electric field strength and ω is the frequency of the emitted electromagnetic wave.

RESULTS OF CALCULATIONS

The autocorrelation function of the total dipole moment of the nitrous oxide molecule N_2O obtained by applying Fourier transform is shown in Fig. 1a. The mutual compensation of a long sign-alternating “tail” of this function is indicative of the reliability of the spectral properties of the gases calculated on its base. The absorption coefficient $\alpha(\omega)$ calculated using the recovered autocorrelation functions (curves 1–5) are shown in Fig. 1b, together with the Earth's emission spectrum calculated on the assumption that the Earth's surface radiates as a black body with a temperature of 288 K (curve 6). Note that the HITRAN data [6] are mostly laboratory measurements, unrelated to actual atmospheric conditions. In this case, it is necessary to adjust the obtained $\alpha(\omega)$ spectra (and $P(\omega)$ dependence) so as to make them suitable for calculating the properties of greenhouse gases in the real atmosphere. It makes sense to assume that all the molecules of the greenhouse gases present in the atmosphere are involved in radiative energy exchange. In this case, the intensity of radiation absorption is determined not only by the dielectric properties of the molecules involved, but also by the emissivity of the radiation source, i.e., the Earth's radiation frequency spectrum. Each molecule absorbs (emits) radiation at certain characteristic frequencies. The rate of energy transformation by different greenhouse molecules is proportional to the intensity of the source radiation at these characteristic frequencies. Therefore, the nor-

malized Earth's emission spectrum should be used as a weighting factor.

Water vapor absorbs infrared radiation almost continuously throughout the frequency range $0 \leq \omega \leq 3600 \text{ cm}^{-1}$, especially intensely within $0 \leq \omega \leq 2550 \text{ cm}^{-1}$ (Fig. 1b, curve 1). The extended frequency range includes the most intense (experimentally determined [12]) absorption band of water vapor, located at 3400 cm^{-1} . The narrower range encompasses all the absorption bands of the rest of the greenhouse gases considered here. The spectral absorption coefficients $\alpha(\omega)$ are continuous functions of the frequency, with several most intense bands: $681, 1462, 1726,$ and 3551 cm^{-1} (CO_2); $1060, 2118,$ and 3150 cm^{-1} (O_3); split spectral lines at 870 and $971, 1172$ and 1323 cm^{-1} (CH_4); and $920, 1209 \text{ cm}^{-1}$ (N_2O). The spectral absorption coefficient also features weak bands, which do not contribute significantly to the overall absorption, but are important to accurately estimate the greenhouse effect.

Figure 2a shows the spectral radiance $P_{exp}(\omega)$ of the atmosphere within $600\text{--}2000 \text{ cm}^{-1}$, which was recorded in a field experiment in the cold season, at a clear sky and the Sun in the zenith [13]. The measurements were performed using an infrared Fourier spectrometer with a high-resolution of 0.35 cm^{-1} . There are the emission bands of all the major greenhouse gases in this range. As can be seen from Fig. 2a, the emission spectrum of atmospheric CO_2 spans a low-frequency region, which includes approximately one seventh of the intensity of the Earth's thermal radiation. The remaining six sevenths of the intensity of the Earth's emission spectrum fall on the frequency range of the emission of the other gases ($\text{O}_3, \text{N}_2\text{O}, \text{CH}_4,$ and H_2O). Despite the fact that the integrated spectral radiance of CO_2 is almost 2.5 times greater than that of the other gases, carbon dioxide does not produce highly effective radiation, since the maximum of its emission spectrum is shifted to lower frequency by $\sim 380 \text{ cm}^{-1}$ relative to the maximum of the Earth's emission spectrum, with the ratio of the frequencies corresponding to the extrema of these spectra being close to 0.63. The absorption of infrared radiation by gas molecules is a complex physical process. The average frequency of emission for CO_2 is 1.6 times lower than that of the other considered gases. Therefore, the energy efficiency of the resulting CO_2 emission, proportional to $\bar{\omega}$, is almost five times lower than that of the other gases.

The IR spectral radiance $P(\omega)$ in the frequency range $0 \leq \omega \leq 3600 \text{ cm}^{-1}$, also calculated from the recovered autocorrelation function of the total dipole moment of gas molecules, are displayed in Fig. 2b (curves 1–5). For water vapor (curve 1), the spectrum is continuous over the entire range and rather jagged, unlike the emission spectra of the other greenhouse gases, which exhibit from 3 to 5 sufficiently well-resolved peaks. The main bands of the emission spec-

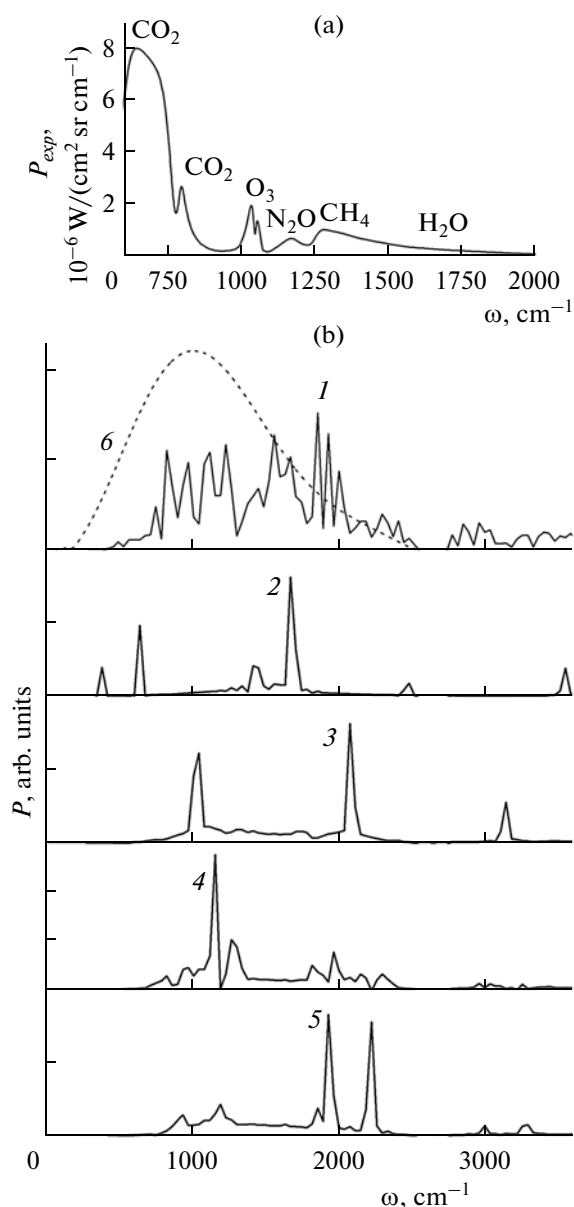


Fig. 2. (a) Measured $P_{exp}(\omega)$ [13] and (b) calculated $P(\omega)$ IR spectral radiance of the greenhouse gases: (1) H_2O , (2) CO_2 , (3) O_3 , (4) CH_4 , (5) N_2O ; (6) Earth's thermal radiation spectrum at $T = 280 \text{ K}$.

tra of the investigated gases fall on the frequencies in the Earth's radiation range: 1887 and 1947 cm^{-1} for H_2O , 659 and 1681 cm^{-1} for CO_2 , 2093 cm^{-1} for O_3 , 1174 cm^{-1} for CH_4 , and 1948 and 2238 cm^{-1} for N_2O . Curve 6 shows the Earth's thermal radiation spectrum at $T = 280 \text{ K}$.

Additional bands in the calculated radiation spectrum can arise due to imperfections of data processing methods, effects of overlapping of the spectra of different gases, as well as due to differences in the conditions of real physical experiments and laboratory measurements, the data of which given in the HITRAN data-

Table 2. Measured values of the radiation flux for a number of IR emission bands of the greenhouse gases

Greenhouse gas	Emission band, cm^{-1}	Radiation flux, W/m^2
H ₂ O	all bands	303.8
CO ₂	all bands	30.9–37.3
CH ₄	1200–1400	1.0–1.2
N ₂ O	1200–1300	1.1–1.3
O ₃	900–1100	3.0–3.3

base. These effects are introduced through the reconstructed (from laboratory measurements) autocorrelation functions of the total dipole moment of gas systems.

Data of atmospheric measurements of the radiation flux for some bands of the emission spectra of greenhouse gases are listed in Table 2. The measurements were carried out on a winter day under clear-sky conditions in Ontario (Canada) for CO₂, CH₄, N₂O, and O₃ [14] and in sub-Arctic latitudes in winter and summer for H₂O [15]. That the local values of the radiation flux differ from the estimates of radiative forcing given above is due to the fact that the measurements were performed on the ground, while the value of radiative forcing was given in the introduction refers to the upper boundary of the atmosphere. In addition, a significant role is played by the duration of experimental measurements. As can be seen, H₂O and CO₂ exhibit broad spectra, producing an intense radiation flux, while the emission spectra of CH₄, N₂O, and O₃ feature a single strong band.

The ratio of the integrated spectral radiances of the considered greenhouse gases in the frequency range $0 \leq \omega \leq 3600 \text{ cm}^{-1}$ to the integrated spectral radiance of carbon dioxide (the gas was chosen as the standard as the most regulated and most abundant in the atmosphere after water vapor) is shown in Fig. 3a (line 1). An analysis of the relative intensity of radiation showed that water vapor has the highest emissivity (which characterizes it as a potent greenhouse gas), whereas ozone (the main function of which is protection from ultraviolet radiation, not the greenhouse effect) exhibits the least. These characteristics are not related to the concentrations of the gases, being determined solely by the structure and electronic properties of their molecules. Next, using the same procedure of superimposing the Earth's thermal radiation spectrum (Fig. 1b, curve 6) and calculating the integrated spectral radiance in the range limited by the Earth's emission spectrum of ($0 \leq \omega \leq 2550 \text{ cm}^{-1}$), we plotted line 3 in Fig. 3a. The form of this dependence is close to that of line 1, except that the relative intensity of water vapor radiation decreased slightly, whereas that of nitrous oxide increased. With respect to CO₂, only ozone proved to be less efficient emitter ($J_{P(\text{O}_3)}/J_{P(\text{CO}_2)} < 1$),

whereas methane and nitrous oxide manifest themselves here as greenhouse gases potentially more dangerous (due to a rapid growth of their concentrations in the atmosphere) than carbon dioxide. Straight lines 2 and 4 represent the average ratio of the integrated spectral radiances of the four considered gases for both cases.

Figure 3b displays the ratio of the integrated spectral radiances of greenhouse gases with consideration for their concentrations C_{GHG} and the CO₂ concentra-

tion C_{CO_2} : $\frac{J_{P(\text{GHG})} C_{\text{GHG}}}{J_{P(\text{CO}_2)} C_{\text{CO}_2}}$ (lines 1 and 3). In this case, the

greenhouse gases will be obviously ranked depending on their concentrations (Table 1). A noticeable difference in the values represented by lines 1 and 3 (characterizing two frequency ranges) is observed only for water vapor. Lines 2 and 4 show the average values of the considered parameter for the four gases.

When calculating the criterion of efficiency of a greenhouse gas, it is important not only to know at which frequencies and how intensely electromagnetic radiation is absorbed, but also have information on the interaction mechanism between the molecule and the absorbed energy. Most of the absorbed energy must be reemitted. If the frequency at which the stored energy is reemitted is lower than the absorption frequency, the molecules will emit spontaneously. This mechanism is operative for the vast majority of greenhouse gases. Another important point is how fast reradiation occurs. The faster the gas molecule emits the stored energy, the sooner it is ready to accept a new portion of electromagnetic radiation, and so the more effective this greenhouse gas is. Thus, in determining the effectiveness of a greenhouse gas, it is important to know not only the absorbed energy but also the rate of transfer of electromagnetic radiation. A gas that intensely absorbs light and reemits it quickly is effective. Calculation of the infrared spectral absorption coefficient makes it possible to determine the integrated spectral absorption coefficient I_α . Knowledge of the integrated spectral radiance J_p and integrated spectral absorption coefficient I_α of the gases enables to calculate the absolute efficiency of greenhouse gases: $\beta_{P\alpha} = J_p I_\alpha$. We will consider the values of J_p and I_α with respect to the intensities of absorption $I_{\alpha(\text{CO}_2)}$, and emission $J_{P(\text{CO}_2)}$, of carbon dioxide and define the relative efficiency of greenhouse gases as

$$\beta = \frac{J_p}{J_{P(\text{CO}_2)}} \frac{I_\alpha}{I_{\alpha(\text{CO}_2)}}$$

Figure 4 shows the efficiency criterion of greenhouse gases β . The greenhouse gases are ranked in the order of increasing this criterion, with $\beta = 1$ for CO₂. Obviously, the inequalities $\beta > 1$ ($\beta < 1$) signify that the gas is more (less) effective than carbon dioxide in creating the greenhouse effect. It is important to note that

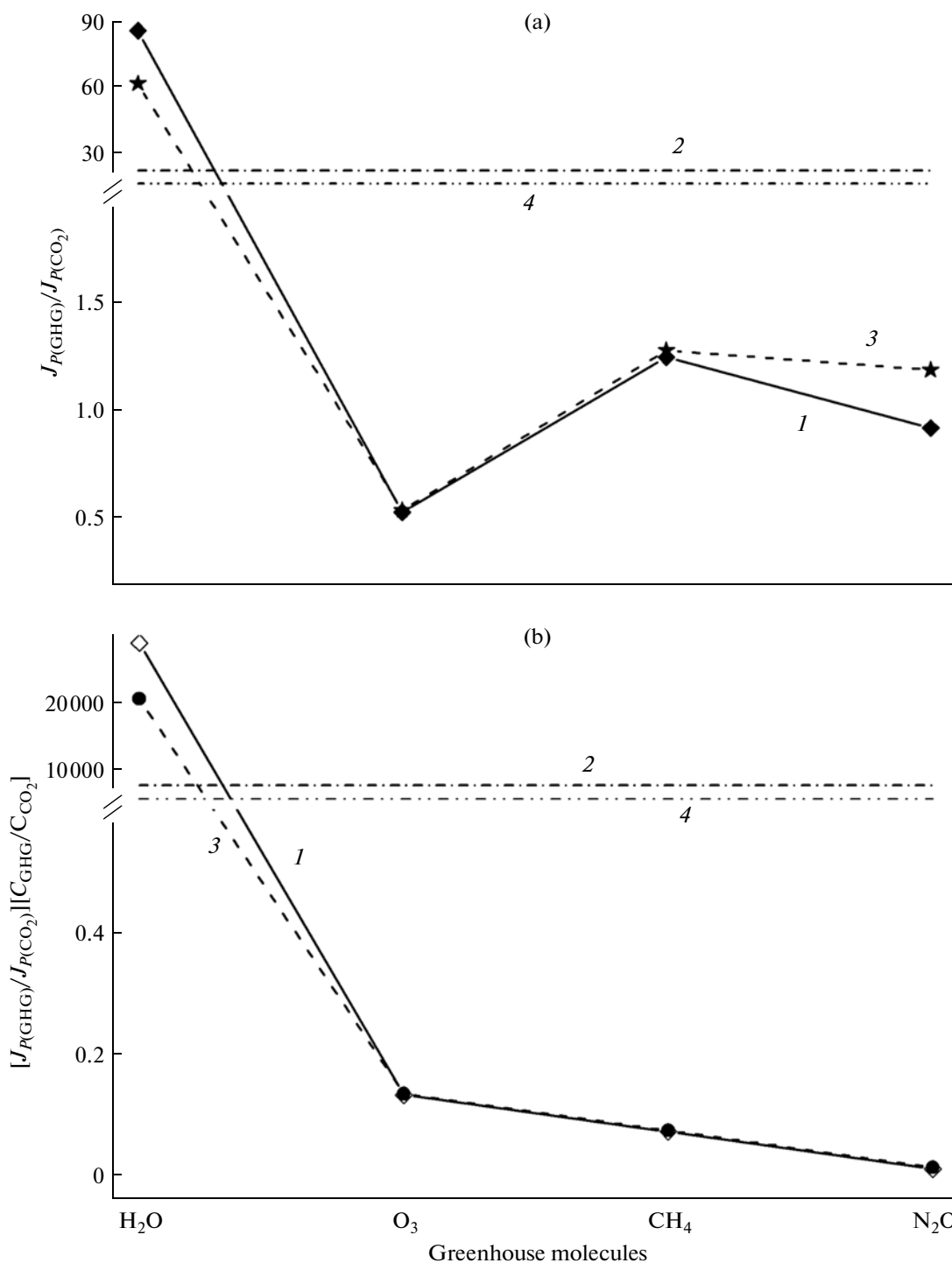


Fig. 3. (a) Ratio of the integrated IR spectral radiance of the greenhouse gases $J_{P(\text{GHG})}$ to the integrated spectral radiance $J_{P(\text{CO}_2)}$ of carbon dioxide: (1) in the frequency range of $0 \leq \omega \leq 3600 \text{ cm}^{-1}$, (3) in the Earth's radiation range ($0 \leq \omega \leq 2550 \text{ cm}^{-1}$); (2, 4) mean values of these quantities; (b) ratio of the integrated IR spectral radiance of the greenhouse gases with consideration for the concentrations of the studied gases. Notations 1–4 have the same meaning as in Fig. 3a.

the group of strong greenhouse gases includes not only water vapor and carbon dioxide, but also methane.

As noted above, the HITRAN data on the IR absorption, obtained in laboratory experiments at

room temperature, are practically unrelated to actual atmospheric conditions. To assess the real contribution of each of the studied gases to the greenhouse effect more accurately, we considered the altitude pro-

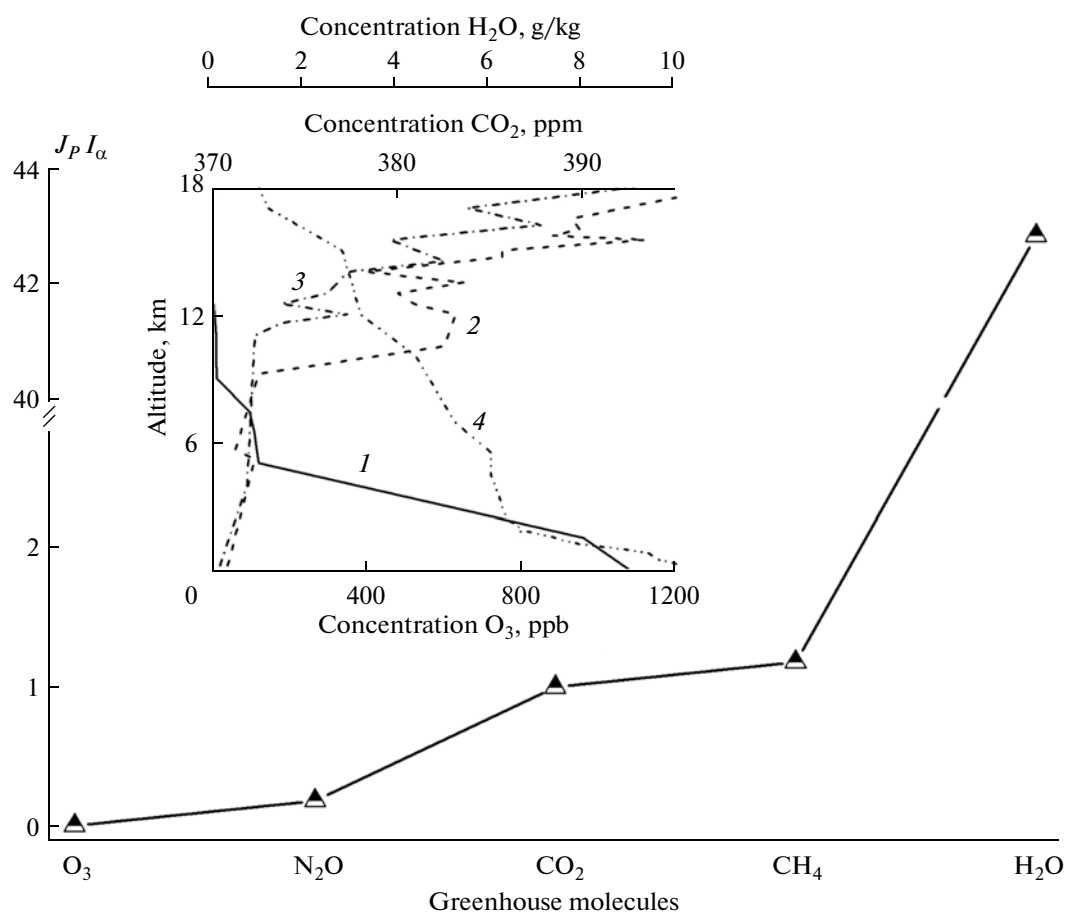


Fig. 4. Criterion of greenhouse efficiency $J_p I_\alpha$ of the studied atmospheric gases. The inset shows the altitude concentration profiles of various greenhouse gases: (1) water vapor [16], (2) ozone in winter [17], (3) ozone in summer [17], (4) carbon dioxide [18].

files of their concentrations. The inset in Fig. 4 shows the altitude profiles of the concentrations of the main greenhouse gases in the troposphere: water vapor (curve 1) [16], ozone during winter (curve 2) and summer (curve 3) [17], carbon dioxide (curve 4) [18]. The H_2O concentration decreases very rapidly with increasing height. The opposite picture is observed for ozone: the troposphere contains only 5% of this gas, with the intensive growth of its concentration starting an altitude of 10–12 km; the maximum concentration occurs at a height of 20–25 km. The concentrations of CO_2 , N_2O , and CH_4 gradually decrease with increasing altitude. The emission–absorption activity of greenhouse gases in the troposphere affects the energy balance of the Earth.

CONCLUSIONS

Extraction of the contribution of each greenhouse gas to the radiative forcing is often difficult because of overlapping effects. In other words, different gases can absorb radiation at the same wavelength. The efficiency criterion of IR absorption and emission introduced in the present work characterizes the efficiency

of radiation propagation. The radiative forcing is a parameter that describes the radiation emission power per m^2 , whereas the proposed quantity β characterizes the relationship between the intensities of emission and absorption of gases with consideration given to their concentrations. According to proposed criterion, the relative efficiencies of the atmospheric greenhouse gases set in the order (from strong to weak): H_2O , CH_4 , CO_2 , N_2O , and O_3 . As can be seen, all the gases, except for ozone, are more effective emitters than CO_2 ($J_{P(\text{GHG})}/J_{P(\text{CO}_2)} > 1$). It should be emphasized that methane and nitrous oxide are potentially more dangerous greenhouse gases.

Note also that, in discussing the growing influence of greenhouse gases on the change in the energy balance of the Earth's atmosphere, the contribution of carbon dioxide as a dominant greenhouse gas of anthropogenic origin is very often overestimated. Estimates of the contribution of water vapor to the greenhouse effect are mixed because of the effect of clouds, which are mostly located at altitudes 1.5–3.0 km, a layer within which up to 60% water vapor occurs. At the same time, the role of methane is underestimated.

In recent years, its concentration increases much faster (up to 1.5% per year) as compared to CO₂ (1.1% per year). The retreat of the permafrost border and melting of wetlands are processes that results in release of methane over vast areas, particularly in Western and Eastern Siberia. A contribution also comes from ever-increasing rice fields and areas of oil production. If the current level of methane concentration doubles, the surface temperature will increase by 0.3 K, which will invariably affect the energy balance of the planet. Therefore, a monitoring and regulation of emissions of not only CO₂, but also other greenhouse gases (CH₄, N₂O, and O₃), is needed.

REFERENCES

1. A. V. Eliseev, *Izv. Atmos. Ocean. Phys.* **44**, 279 (2008).
2. D. J. Hofmann, J. H. Butler, E. J. Dlugokencky, et al., *Tellus B* **58**, 614 (2006).
3. World Meteorological Organization, *Greenhouse Gas Bull.* **3**, 4 (2007).
4. International Panel on Climate Change, *Climate Change 2007: The Physical Science Basis* (Cambridge Univ. Press, Cambridge, UK, 2007).
5. R. M. Strat, *Acc. Chem. Res.* **28**, 201 (1995).
6. T. Keyes, *J. Chem. Phys.* **104**, 9349 (1996).
7. L. S. Rothman, I. E. Gordon, A. Barbe, et al., *J. Quant. Spectrosc. Radiat. Transf.* **110**, 533 (2009).
8. J. T. Kindt and C. A. Schmuttenmaer, *J. Chem. Phys.* **106**, 4389 (1997).
9. F. Bresme, *J. Chem. Phys.* **115**, 7564 (2001).
10. M. Neumann, *J. Chem. Phys.* **82**, 5663 (1985).
11. *Physical Encyclopedia*, Ed. by A. M. Prokhorov (Sov. Entsiklopediya, Moscow, 1988) [in Russian].
12. P. L. Goggin and C. Carr, *Water and Aqueous Solutions*, Vol. 37 (Adam Hilger, Bristol, Boston, 1986), p. 149.
13. W. F. Evans and E. Puckrin, *J. Clim.* **8**, 3091 (1995).
14. W. F. Evans, E. Puckrin, and T. P. Ackerman, in *Proceedings of the 12th ARM Science Team Meeting* (St.-Petersburg, Florida, 2002), p. 1.
15. T. Matsui and Sr. R. A. Pielke, *Geophys. Res. Lett.* **33**, L11813 (2006).
16. M. N. England, R. A. Ferrare, S. H. Melfi, D. N. Whiteman, and T. A. Clark, *J. Geophys. Res.* **97**, 899 (1992).
17. G. Vaughan, C. Cambridge, L. Dean, and A. W. Phillips, *Atmos. Chem. Phys. Discuss* **4**, 8357 (2004).
18. J. B. Abshire, H. Riris, G. R. Allan, et al., *Tellus B* **62**, 770 (2010).

Translated by V. Smirnov